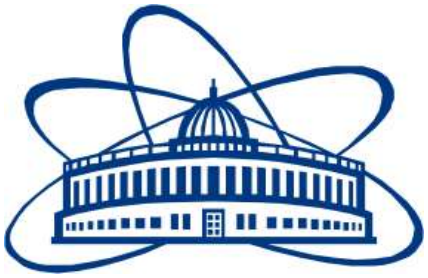

JOINT INSTITUTE FOR NUCLEAR RESEARCH

Dzhelepov Laboratory of Nuclear Problems

Study of charmonium production in Pythia8 and SPDroot

Final report of the START Programme

Supervisor:
Dr. Igor Denisenko

Student:
Anton Anufriev, Russia
Samara University

Participation period:
March 01 – April 25,
Winter Session 2023

Dubna, 2023

1 Abstract

This work investigates charmonia production processes at SPD niaca energies, focusing on η_c and J/ψ.

The approach of creating new processes in Pythia to study η_c meson production with decay into photon pairs is developed in the first part of the work. Results of numerical calculations are presented in the form of classical signal-background picture and in comparison with differential cross sections from the author's previous theoretical work. Comparison of total cross sections from theory and Pythia is also presented.

The second half of the work is related to calculations of J/ψ meson production with $p\bar{p}$ decay in the SpdRoot framework. The main goal of this part of the work is to introduce the features of the framework with "MCTruth"and PID information. Results of numerical calculations were processed by imposing restrictions on candidates in probabilities of protons and antiprotons candidates and phase space. Signal-background image with calculation of efficiency is presented.

2 Introduction

The mega-science "NICA Complex" (fig. 1) project is being implemented at the Joint Institute for Nuclear Research (JINR) in accordance with the Institute's development plans and the Agreement between the Government of the Russian Federation (RF) and the International Intergovernmental Research Organization Joint Institute for Nuclear Research (JINR) on the construction and operation of a complex of superconducting rings on colliding beams of heavy ions NICA – NICA Complex.

The collisions of protons and deuterons with longitudinal and transverse polarization in the energy range up to $\sqrt{S_{NN}} = 27$ GeV and $\sqrt{S_{NN}} = 12.6$ GeV, respectively, with luminosities up to 10^{32} cm$^{-2}s^{-1}$, will be available at the Collider. These conditions will provide priority in the field of the nucleon spin structure research and clarification of the most important questions of the spin origin. [1]

In additional, it is possible to accelerate and collide heavy ions, up to gold ions, in the optimal energy range, from the minimum — in the zone of extracted beams, to the most achievable $\sqrt{S_{NN}} = 11$ GeV (for Au^{+79}, in the nucleon-nucleon center of mass system) at the collider, with an average luminosity of $L = 10^{27}$ cm$^{-2}s^{-1}$, which will allows to study nuclear matter in a state of maximum baryonic density, inaccessible to research in other laboratories of the world.

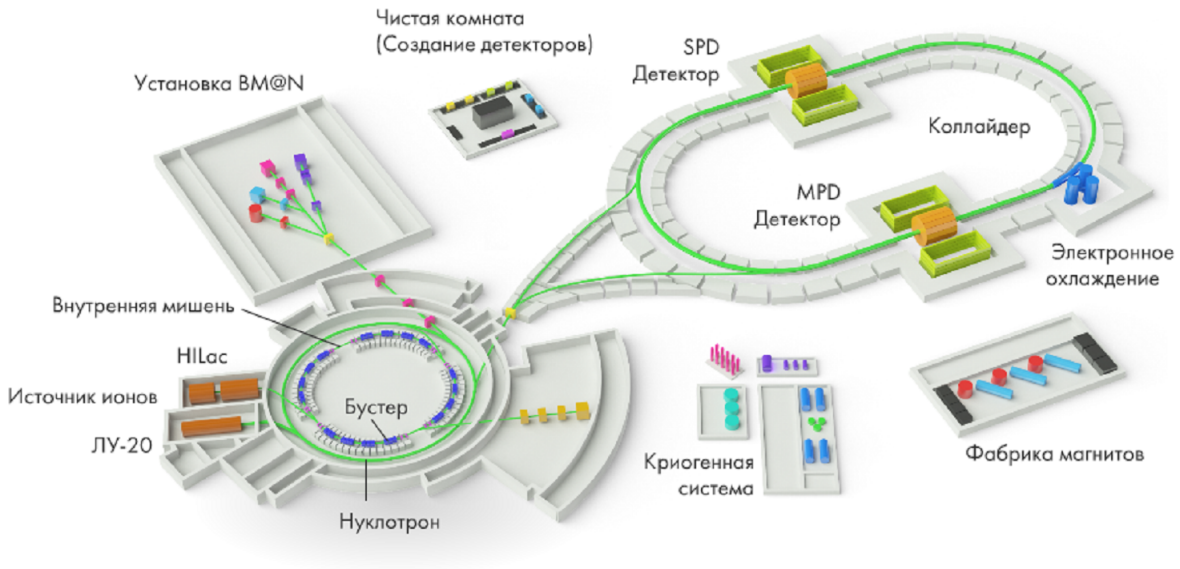

Рис. 1: NICA complex

3 SPD

The SPD (fig. 2) is planned to operate as a universal facility for comprehensive study of the unpolarized and polarized gluon content of the nucleon at large Bjorken-x, using different complementary probes such as: charmonia, open charm and prompt photon production processes. The experiment aims to provide access to the gluon helicity, gluon Sivers and Boer-Mulders PDFs in the nucleon, as well as the gluon transversity distribution tensor PDFs in the deuteron, via the measurement of specific single and double spin asymmetries. [2] The main subsystems of the detector will be discussed on the following pages.

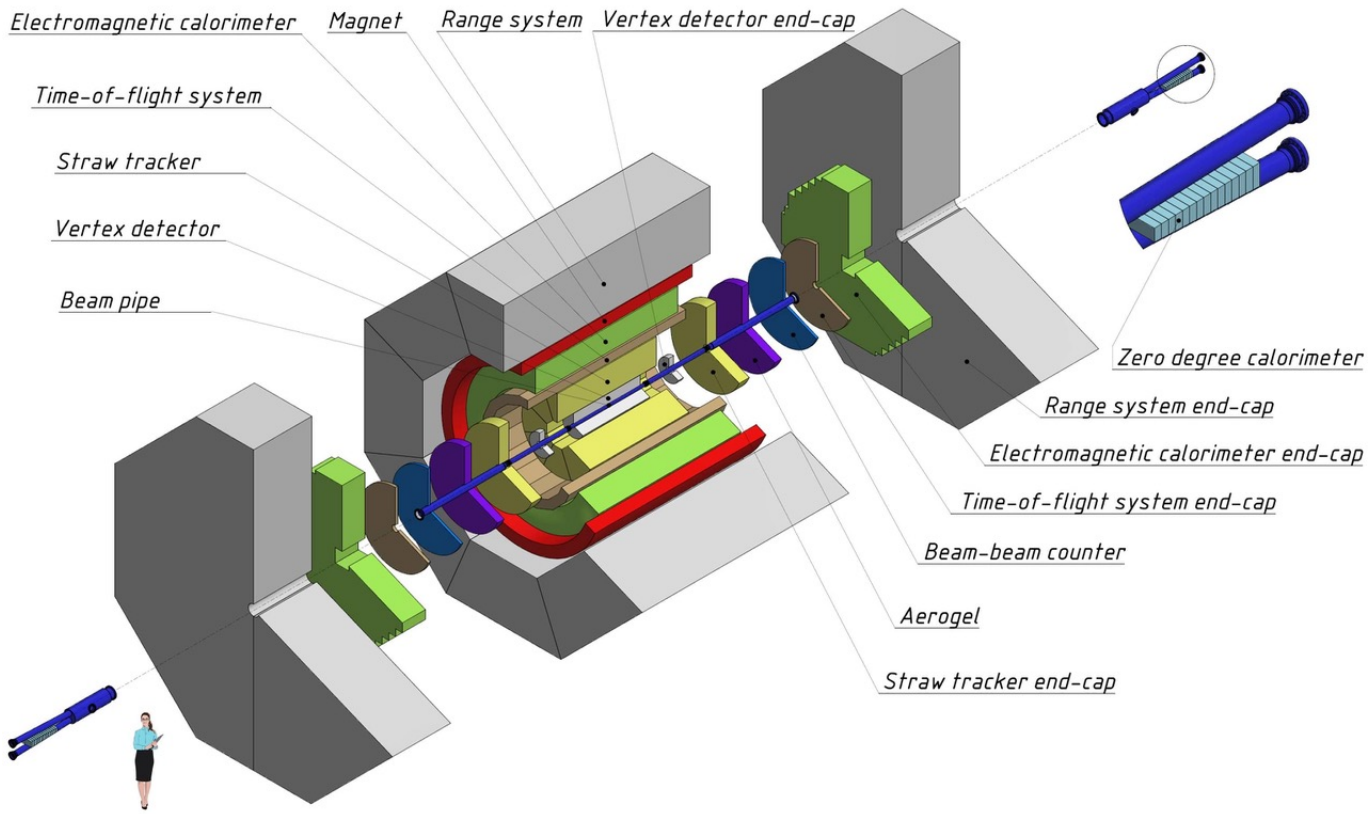

Рис. 2: SPD-detector scheme

3.1 Vertex detector

The SPD Vertex Detector (VD) is a silicon-based part of the spectrometer responsible for precise determination of the primary interaction point and measurement of secondary vertices from the decays of short-lived particles (first of all, D-mesons) [3].The DSSD SVD barrel consists of three layers, based on the Double-Sided Silicon Detectors (approximately 1.9 m^2). The end-cap regions consist of three disks each (approximately 0.22 m^2). The end-cap regions detect particles in the radial region between 32 mm and 250 mm. Each of the three disks is set with a DSSD with concentric (r) strips and radial (ϕ) strips. The SVD has a length of about 1.2 m and covers the region of pseudo-rapidity up to $|\eta| < 2.0$. Each DSSD has a 300-µm thickness and a strip pitch in the range from 95 μm to 281.5 μm. The DSSDs are assembled into detector modules by two detectors per module, forming 18-cm long strips.

3.2 Straw detector

The purpose of Straw Tracker (ST) is to reconstruct tracks of primary and secondary particles with high efficiency, to measure their momenta with high precision based on a track curvature in a magnetic field, and participate in particle identification via energy deposition (dE/dx) measurement. A spatial resolution of ST is expected to be about 150 μm and the drift time is about 120 ns for tubes of 1-cm diameter. The detector is assembled from about 26 000 straw tubes. A single straw tube is manufactured from a thin polyethylene terephthalate (PET) foil, which is welded longitudinally by ultrasonic welding to form a tube. The straw has an active length from 10 cm to 2.7 m and a nominal inner diameter of 9.8 mm. Its inner surface has a metal coating (Cu/Au) to provide electrical conductance on the cathode, while the

electrons, produced in ionization processes, will drift towards the central wire anode.

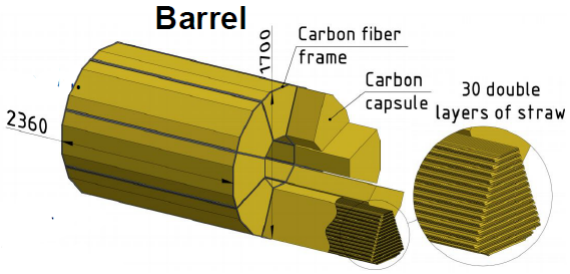

Рис. 3: Straw detector barrel

3.3 Electromagnetic calorimeter

The calorimeter (fig. 4) should meet the criteria imposed by the physical goals of the SPD experiment of different nature and importance. The most important criteria arise from the physical requirements to the accuracies of measurement of energies, trajectories, and timings of photons and electrons. The SPD electromagnetic calorimeter is placed between the Range System and the magnet coils, as shown in Figs.1.2 and 4.1. It consists of a barrel and two end-caps, covering a 4π solid angle. The outer dimensions of the calorimeter are determined by the inner size of the muon system. The thickness of the calorimeter is determined by the required thickness of the active part and the size of the readout block consisting of photodiode and amplifier boards, as well as by the size of the flexible part of the fibers. The SPD experiment imposes the following requirements on the calorimeter characteristics:

— reconstruction of photons and electrons in the energy range from 50 MeV to 10 GeV;
— energy resolution for the above-mentioned particles: $\sim 5\% \sqrt{E[GeV]}$;
— good separation of two-particle showers;
— operation in the magnetic field;
— long-term stability: 2÷3% in a six month period of data taking.

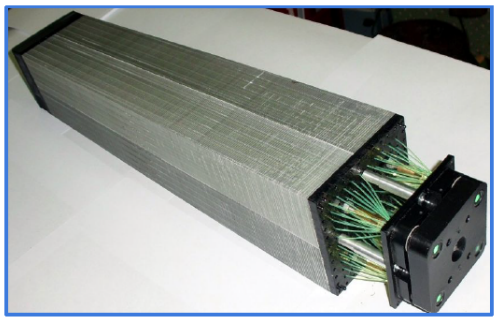

Рис. 4: Electromagnetic calorimeter module prototype

3.4 Particle identification system

Particle identification system consist of two important parts: Time-of-flight (TOF) system and aerogel.

The purpose of the time-of-flight (TOF) system is to discriminate between charged particles of different masses in the momentum range up to a few GeV/c. The TOF system will consist of a barrel and two end-cap parts with an overall active area of 22.6 m^2. The charged particle rate that detector will have to withstand is 0.1 kHz/cm^2 for the barrel. The rate increases rapidly when moving closer to the beam axis. Thus, for the TOF elements located in the end-caps 20 cm off the beam axis, the rate of about 1 kHz/cm^2 is expected (see Fig. 16.1 for details). The MRPC technology is being considered for the TOF detector.

Another option for the system of particle identification is aerogel Cherenkov counters. Aerogel is a synthetic porous ultralight material which has found an application, in particular, as a radiator in Cherenkov counters. Aerogel may have a refractive index in the range between 1.0006 and 1.2, the exact value of the refractive index being specified at the production stage. In fact, aerogel fills the gap in the refractive index values between gases and liquids. This feature of aerogel allows one to use it in Cherenkov counters for particle identification in conditions when other Cherenkov radiators are not applicable, for instance, for π/K separation at the momenta from few hundred MeV/c to about 3 GeV c.

3.5 Range muon system

The Range System of the SPD detector serves for the following purposes: (i) identification of muons in presence of a remarkable hadronic background and (ii) estimation of hadronic energy (coarse hadron calorimetry). It is important to stress that the system is the only device in the SPD setup, which can identify neutrons (by combining its signals with the electromagnetic calorimeter and the inner trackers). Muon identification (PID) is performed via muonic pattern recognition and further matching of the track segments to the tracks inside the magnets. The precise muon momentum definition is performed by the inner trackers in the magnetic field. The Mini Drift Tubes [6] are used in the Range System as tracking detectors providing two-coordinate readout (wires and strips running perpendicularly). Such readout is mostly needed for the events with high track multiplicity and also for the reconstruction of the neutron space angle. The Range System serves as an absorber for hadrons and a 'filter' for muons. It also forms the magnet yoke. It consists of a barrel and two end-caps. Each end-cap, in its turn, consists of an end-cap disk and a plug.

4 Gluon distributions probe with η_c

η_c meson ($^1S_0$ charmonia state) production processes are very interesting for SPD. The factorisation for it has been proven and it is a good probe for gluon parton distribution functions. [7] It is a difficult particle to experiment on. Because of the specific energies, charmonia can be studied on SPD, including η_c. It is important to use some package for modeling it.

4.1 Pythia8 for event generation

In particle physics, the result of a collision between two incoming particles, or the isolated decay of a particle, is called an "event". At the most basic level, an event therefore consists of a number of outgoing particles, as might be recorded in a snapshot taken by an idealised detector, with conservation

laws implying that the summed total energies and momenta of the particles in the final state should be equal to those in the initial state, as should any discrete quantum numbers conserved by the physical process(es) in question. Due to the randomness of quantum processes, the number of outgoing particles and their properties vary from event to event. The probability distributions for these properties can be inferred by studying an ensemble of events in the data. Conversely, given a set of theoretically calculated (or modelled) probability distributions, it is possible to generate ensembles of simulated events to compare with data.

PYTHIA [8] is a programme for the generation of high-energy physics collision events, i.e. the description of high-energy collisions between electrons, protons, photons and heavy nuclei. It contains theory and models for a number of aspects of the physics, including hard and soft interactions, parton distributions, initial and final state parton showers, multiparton interactions, fragmentation and decay. It is largely based on original research, but also borrows many formulae and other knowledge from the literature.

Pythia makes it possible modeling of ${}^3S_1$,${}^3P_J$ and ${}^3D_J$ charmonia states production processes and similar bottomonia states, but limited database of Pythia cannot provide the possibility to model direct η_c production.

4.2 Production of J/Ψ-meson with η_c parameters and decay into γ pairs

Charmonium (preferably η_c) production with decay into only two photons is studied in this part of work. The γ-pair of η_c is considered as signal and other photons as background. "Beams:eCM = 27."gives information about $\sqrt{S}$ in CM system for a generator. The command "441:oneChannel = 1 1 0 22 22"is needed to use only one decay channel in photons. 441 is the id of the J/Ψ particle in the Pythia database. It is important to use a particle data class for changing all specific J/Ψ values on η_c analogs (mass, spin and some other quantum numbers), because η_c production is the main purpose of this job. The command that invokes the process of producing $J/\Psi + g$ from the singlet $c\bar{c}$ state is "Charmonium:gg2ccbar(3S1)[3S1(1)]g=[on,off] where "on"flag corresponds to the $3S1$ singlet state and "off"does not allow other states of the charmonium to be produced. There is possibility to setup Pythia in background generation, usually command "SoftQCD:all=on"is used. It is used to normalise number of events summarised number of events on the year. There is a simple formula $N_{year} = \sigma LT$, where σ - cross section of a process evaluated by Pythia or cross section from theoretical calculations (this will be discussed later), L - luminosity of the collider = $10^{-32}\frac{1}{cm^2 \cdot s}$, T - total working time per year = 10^7 s.

The number of events as a function of the diphoton invariant mass (here we are talking about all possible photon pairs from the background and photon pairs from the charmonium) is shown on graphs 5 (singlet) and 6 (octet).

4.3 Production of η_c-meson with using of internal Pythia ${}^3S_1$-state production process

There is a description of using "Charmonium:states(3S1)=[441,...]"type of command. It is important to note only the first flag in the braces, because the [on,off] flag in the command from the previous paragraph

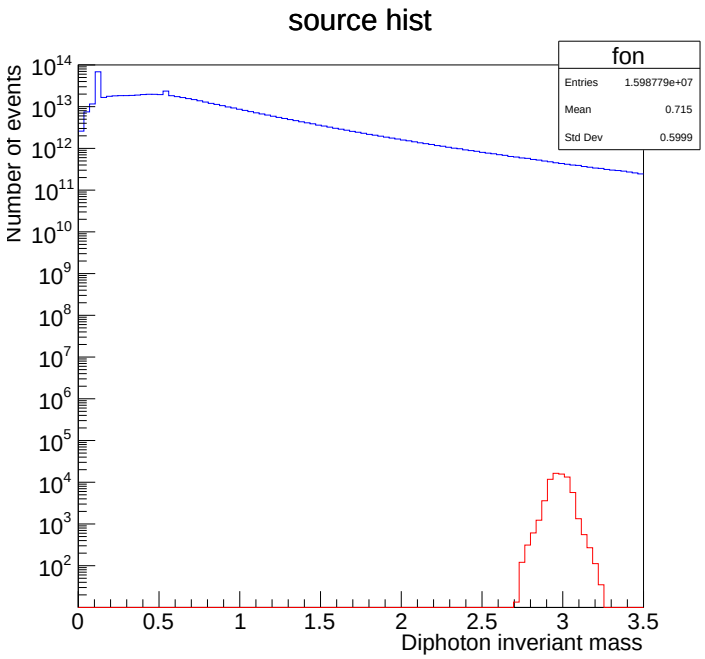

Рис. 5: Event distribution of singlet J/Ψ-meson with η_c parameters production with [0-3.5] invariant mass range

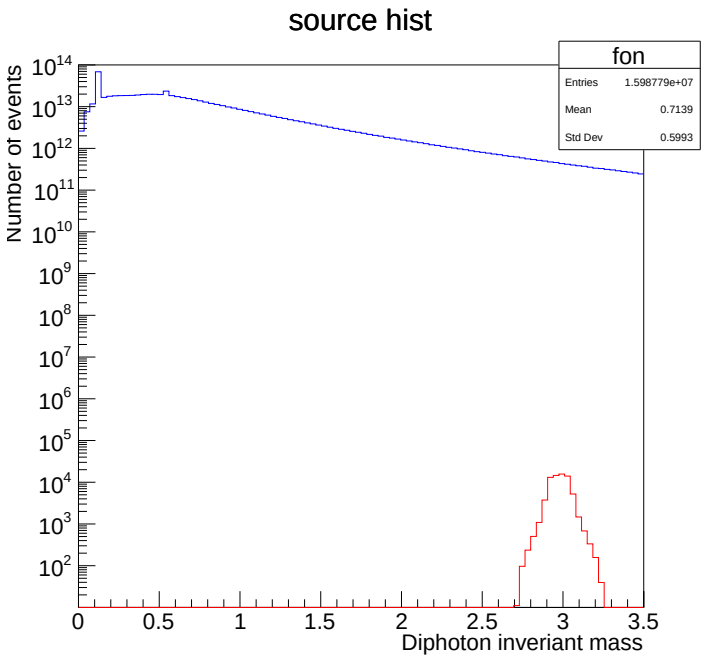

Рис. 6: Event distribution of octet J/Ψ-meson with η_c parameters production with [0-3.5] invariant mass range

allows to create only charmonium with id 441, which is η_c-meson in pdg notation. [9]. Also the command "Charmonium:O(3S1)[3S1(1)]=[0.387,...]"was used for the singlet η_c LDME (is equal to $\frac{<^3S_1(1)>}{3}$) and "Charmonium:O(3S1)[3S1(8)]=[0. 0022,...]"(it is equal to $\frac{<^3S_1(8)>}{3}$ with $<^3 S_1(8) >$ value, which fit in [10] paper) for octet LDME. The η_c decays into photon pairs as before. Plots 7 show the distribution of events by photon pair invariant mass with colour singlet $^3S_1$ state production and 8 with octet production.

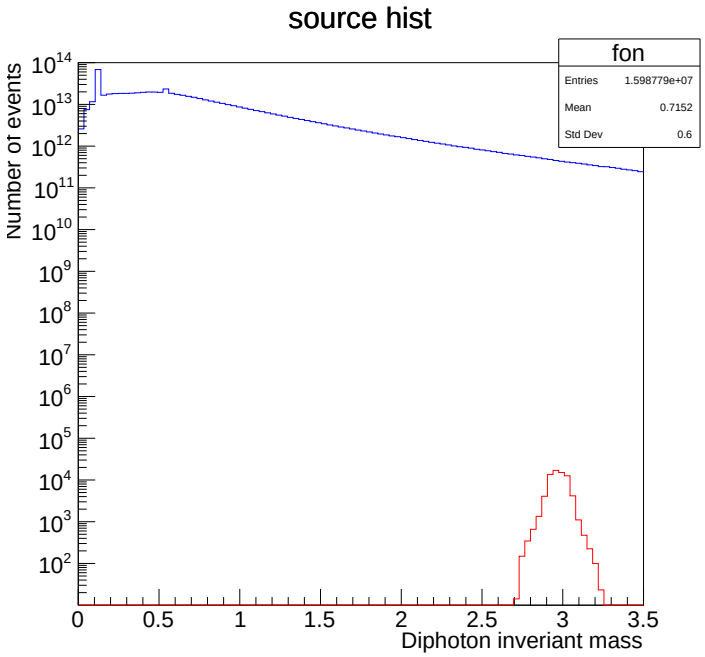

Рис. 7: Event distribution of singlet η_c production from $^3S_1$ process with [0-3.5] invariant mass range

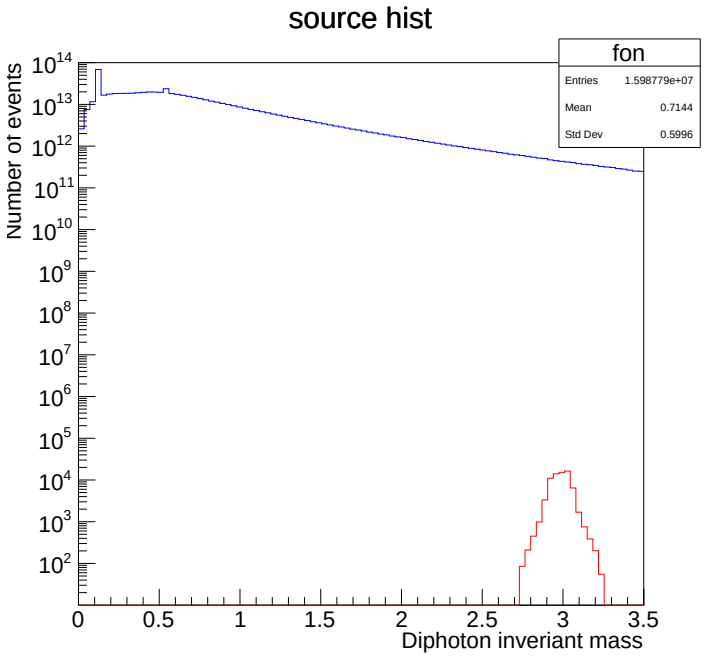

Рис. 8: Event distribution of octet η_c production from $^3S_1$ process with [0-3.5] invariant mass range

4.4 Creating a new processes in Pythia

There is the possibility of using Pythia in advance because the package structure is based on C++ OOP with a very clear class-objects structure. There is enough information in the manual, header files and files with .c extension to create your own classes. You should use the SigmaProcess class for this purpose. There are implementations of Sigma1Process, Sigma2Process and Sigma3Process for $2 \to 1$, $2 \to 2$ and $2 \to 3$ processes. Inheriting from one of these classes for a new class will make a new process. [11]. You can give information about squared matrix elements (or differential cross section), decays and colour flow of this process to describe the new class.

In some cases you may need to create resonance particles. Then you should use ResonanceWidth class and "isResonance()=true"command in particle data if you need.

Example main22.c from Pythia studied to understand the use of this method.

4.5 Simulations of $g + g \to \eta_c + g$ process with η_c-decay in γ-pair

All commands from the J/Ψ subsection are used with a new command - creating a Sigma2Process inheritance class object. Then I have directly produced η_c-meson and gluon. Also used is a $\frac{d\sigma}{d\hat{t}}$ which was found with the help of Wolfram Mathematica package and compared with formula in 1987 article by Gastmans et al. [12]

$$\frac{d\sigma}{dt} = \frac{\pi\alpha_s^3 R_0^2}{8M_{\eta_c}\hat{s}^2}\left(\frac{M_{\eta_c}^4 - \hat{s}^2 - \hat{t}^2 - \hat{u}^2}{(\hat{s} - M_{\eta_c}^2)(\hat{t} - M_{\eta_c}^2)(\hat{u} - M_{\eta_c}^2)}\right)^2 \frac{M_{\eta_c}^8 + \hat{s}^4 + \hat{t}^4 + \hat{u}^4}{\hat{s}\hat{t}\hat{u}} \tag{1}$$

Graphic 9 show distribution of events by photons invariant mass with $\eta_c + g$ production.

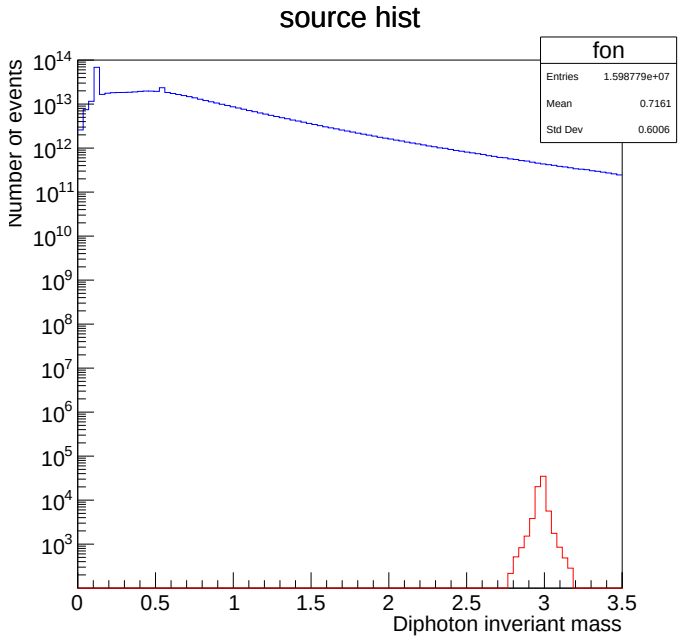

Рис. 9: Event distribution of $g + g \to \eta_c + g$ process with [0-3.5] invariant mass range

4.6 Simulations of $g + g \to \eta_c$ process

Class Sigma1Process allows to create $2 - 1$ process. It is possible by using squared Matrix elements for this process in analogy with octet η_c production from paper [13]:

$$|\bar{M}|^2 = \frac{2}{9}\pi^2\alpha_s^2\frac{<^1 S_0(1) >}{M} \tag{2}$$

There are distribution of events by photons invariant mass with $\eta_c + g$ production on picture 10.

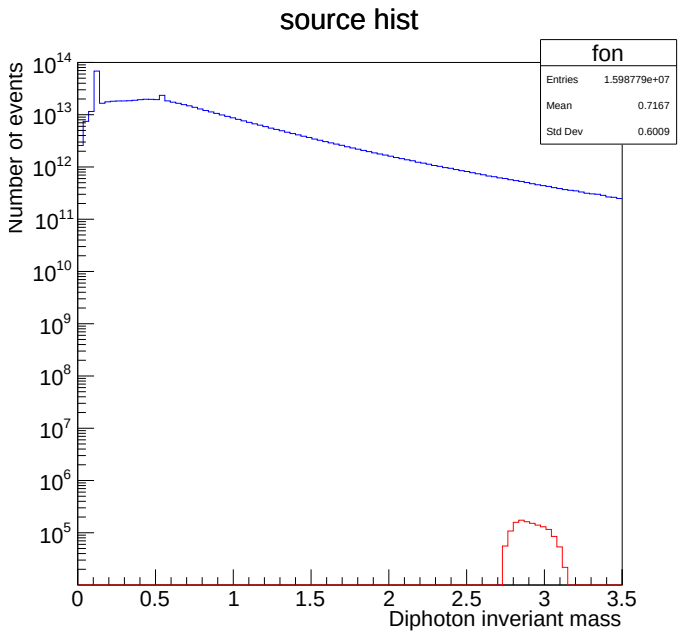

Рис. 10: Event distribution of $g + g \to \eta_c$ process with [0-3.5] invariant mass range

4.7 Simulations of $g + g \to \eta_c \to \gamma + \gamma$ process

η_c is considered as a particle with very small lifetime value (not so rough approximation) in this process (fig. 11), i.e. as a resonance. Also width of η_c-decays $\Gamma_{\eta_c \to > g+g}$ and $\Gamma_{\eta_c \to \gamma+\gamma}$ is used.

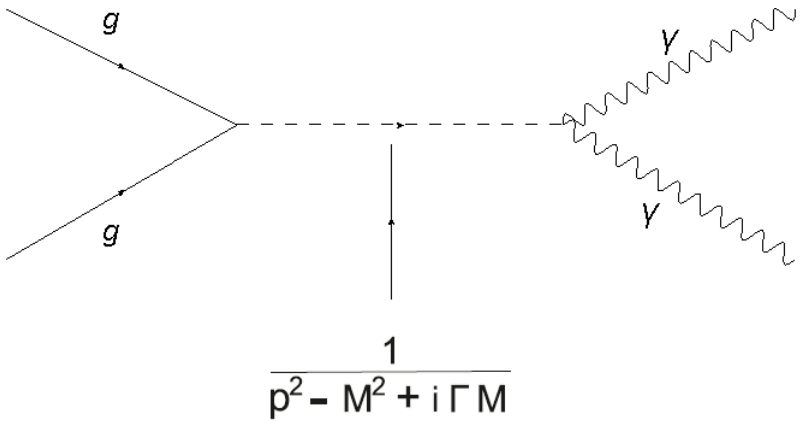

Рис. 11: Feynman amplitudes of process, η_c is propagator in Breit-wigner form

Formula of squared matrix elements is

$$|\bar{M}|^2 = \frac{8M_{\eta_c}^2 \Gamma_{gg}\Gamma_{\gamma\gamma}}{256((\hat{s}-M_{\eta_c}^2)^2 + M_{\eta_c}^2\Gamma^2/4)} \tag{3}$$

with $\Gamma_{\gamma\gamma} = 12e_c^4\alpha_{em}^2\frac{|R(0)^2|}{M_{\eta c}^2}$ and $\Gamma_{gg} = \frac{2}{9}\alpha_s^2\frac{|R(0)^2|}{M_{\eta c}^2}$
Graphic 12 shows distributions of events by diphoton invariant mass.

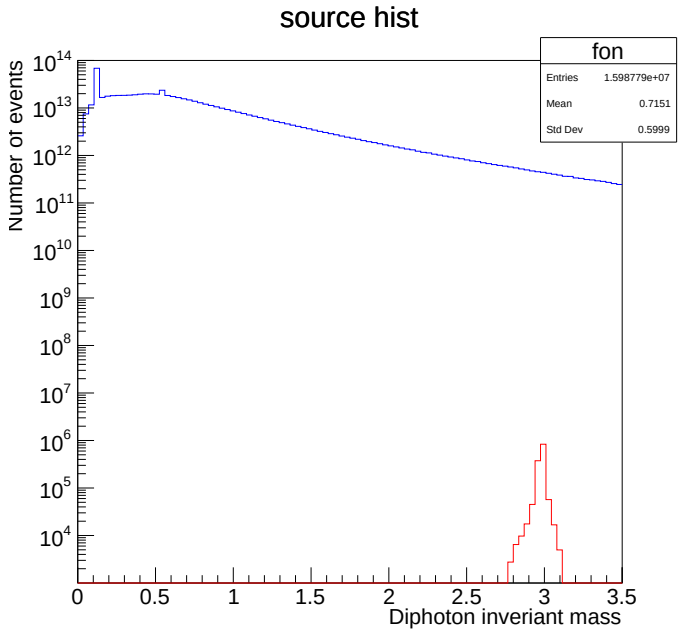

Рис. 12: Event distribution of $g + g \to \eta_c \to \gamma + \gamma$ process with [0-3.5] invariant mass range

4.8 Evaluated cross sections comparison with theoretical calculations

I have calculated most of these processes in my earlier theoretical work. Some of these calculations are included in the paper [14]. For theoretical calculations we derive basic formulas for kinematics, Feynman amplitudes, differential and integrated cross sections. Then the CUBA integrator [15] is used to compute multidimensional integrals in the main formula. Collinear Parton Model (CPM) [16] and Generalised Parton Model (GPM) [17] are basic models for calculations. There are calculations without FSR, ISR, MPI, hadronisation and decay modes in Pythia for this comparison.

The differential cross section of the transverse momentum determination in Pythia with the transverse momentum of the charmonium on the X-axis (red curve) in comparison with the theoretical calculations (blue curve) is shown on the pictures with number 13 for $g + g \to \eta_c + g$, 14 for $g + g \to \eta_c$ and 15 for $g + g \to \eta_c \to \gamma + \gamma$ processes.

Because of the $g+g \to \eta_c+g$ process computed in CPM, the Pythia program has a "BeamRemnants:primordial which is used to switch off the dependence of the calculations on the transverse momenta of the initial partons. This is important for GPM. Two other processes are calculated in this model. I use the command "BeamRemnants:primordialKThard=1.2"to find the correspondence between theoretical and Pythia calculations

It is interesting to compare total cross section of the above process in theoretical calculations with Pythia predictions. This comparison is shown in the table.

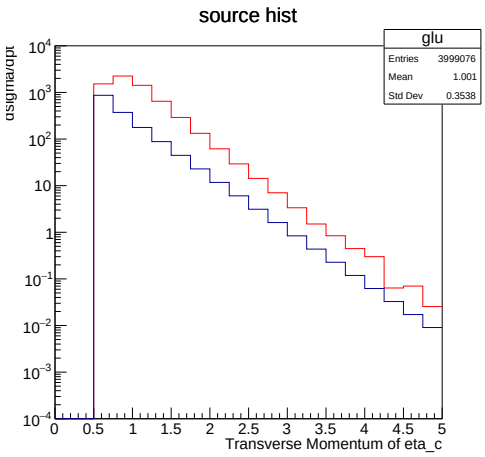

Рис. 13: $\frac{d\sigma}{dp_T}$ distribution of $g+g \to \eta_c + g$ process with [0-5] transverse momentum range

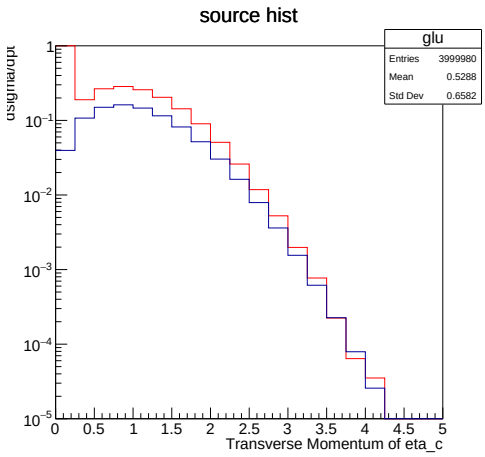

Рис. 14: $\frac{d\sigma}{dp_T}$ distribution of $g + g \to \eta_c$ process with [0-5] transverse momentum range

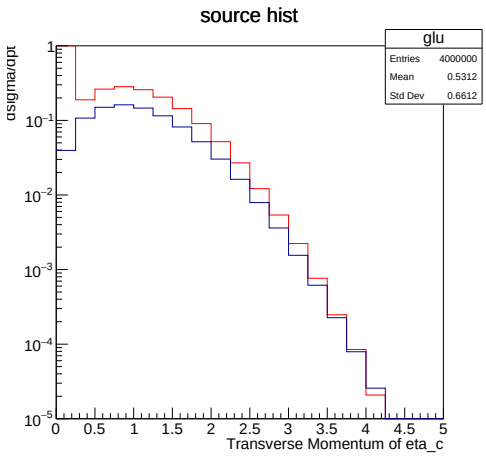

Рис. 15: $\frac{d\sigma}{dp_T}$ distribution of $g + g \to \eta_c \to \gamma + \gamma$ process with [0-5] transverse momentum range

process $g + g \to ...$	Total σ in theory	Total σ in Pythia8
$\eta_c + g$	398 nb (CPM)	419 nb
η_c	1283,895 nb (GPM)	2230 nb
$\eta_c \to \gamma + \gamma$	0.22 nb (GPM)	0.46 nb

It is important that in $g+g \to \eta_c \to \gamma+\gamma$ process integrated cross section taking into account branching ratio of η_c decay into photons. $Br(\eta_c \to \gamma + \gamma) = 1.78 \cdot 10^{-4}$.

5 Search for η_c in $J/\psi \to p\bar{p}$ decay process

η_c have various decay channels, except above-mentioned into photon pair. We can find η_c in $p\bar{p}$ decay channel, however J/ψ has the same final decay state with a more little branching and much less width. From LHCb results [18] it is known we have some chances to find η_c in pp collisions only if J/ψ is founded.

So, decay of J/ψ to $p\bar{p}$ can be a reference process of η_c.

5.1 SPDRoot simulations

SPDroot is a framework specifically designed for SPD NICA [19]. It is based on the FairRoot package [20], which provides basic classes that allow users to construct their detectors and/or analysis tasks in an easy way, it also provides some general functionality like track visualisation. The geometry of the detectors is modelled using the Geant4 package [21] and the CERN package ROOT [22] provides the possibility to build a plot.

Because of a very large number of classes in SPDroot, it is possible to simulate interesting processes with very small scales not far from the primary vertex of the collision in Pythia 8, using Geant4 with actual geometry of all SPD detector parts to "catch"Pythia events. Pythia 8 is also used as a decayer for Geant4 modelling.

After the simulation, we only have the electronic signal from the virtual devices of the SPD detector, which can be reconstructed into information that we can extract from the real experiment.

The third file - analysis - allows us to find tracks and vertices of particles and also to perform identification of candidate particles.

It uses only a small part of the real functionality of SPDroot for this task because of the time constraints we have.

5.2 Peak widths comparison for $p\bar{p}$, $\mu^+\mu^-$ and $2(K^+K^-)$ from J/ψ decay

It is interesting to find out how the width of J/ψ peak depends on the type of particles in the final state. Because of that the first task of the work is to make a simulation, reconstruction and analysis for proton-antiproton, muon-antimuon pairs from J/ψ decay. It is also interesting to see the results of this work for the $J/\psi \to 2(K^+K^-)$ decay. For the first task it was possible to use MCTruth (where after reconstructions MCParticles class gives us access to Monte Carlo events information). It will be forbidden for the next tasks, because in the real world we don't have "events just a set of detector signals.

All signal calculations in this paper include 2000 events in the simulation file due to hardware limitations.

All distributions by invariant masses of particles are shown in Figure 16.

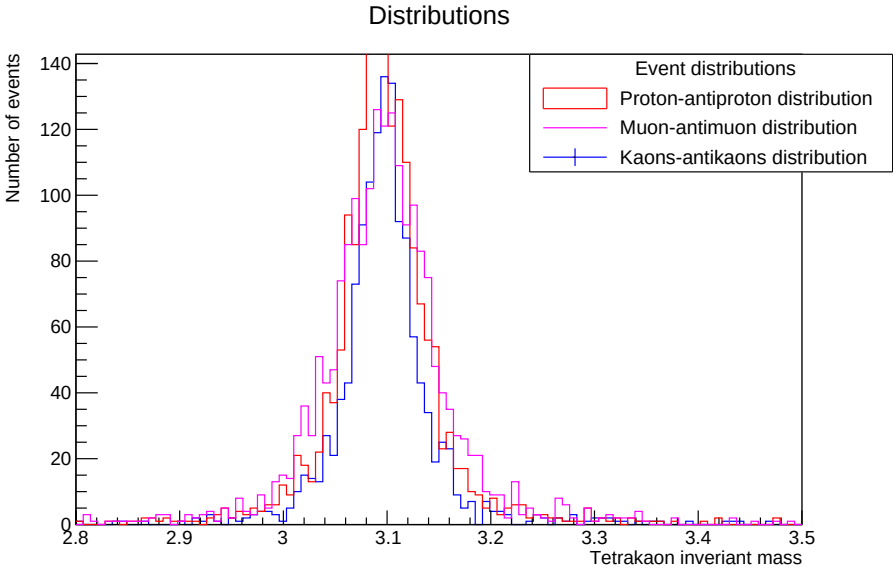

Рис. 16: Event distribution of $g + g \to J/\psi + g$ process with decay into $p\bar{p}$ (red curve on graph), $\mu^+\mu^-$ (magenta) and $2(K^+K^-)$ (blue curve)

For the right-hand comparison of these decays, fitting class TF1 was used in ROOT. Sum of two Gaussians with the same expectation mean values and different widths was chosen as a fitting function. After fitting weights of distributions was founded by formula:

$$w_1 = \frac{N_1}{N_1 + N_2}$$

$$w_2 = \frac{N_2}{N_1 + N_2},$$

where N_1 and N_2 - constant multipliers of first and second Gaussian. Total standard deviation, which is equal to width of event distribution, was obtained by formula:

$$\sigma = \sqrt{w_1^2\sigma_1^2 + w_2^2\sigma_2^2},$$

where σ_1^2 and σ_2^2 is first and second Gaussian variances.

This values for different decays is $\sigma_{p\bar{p}} = 0.0331432, \sigma_{\mu^+\mu^-} = 0.0421808, \sigma_{2(K^+K^-)} = 0.0306243$

A comparison of the Gaussian fit is shown in Figure 17.

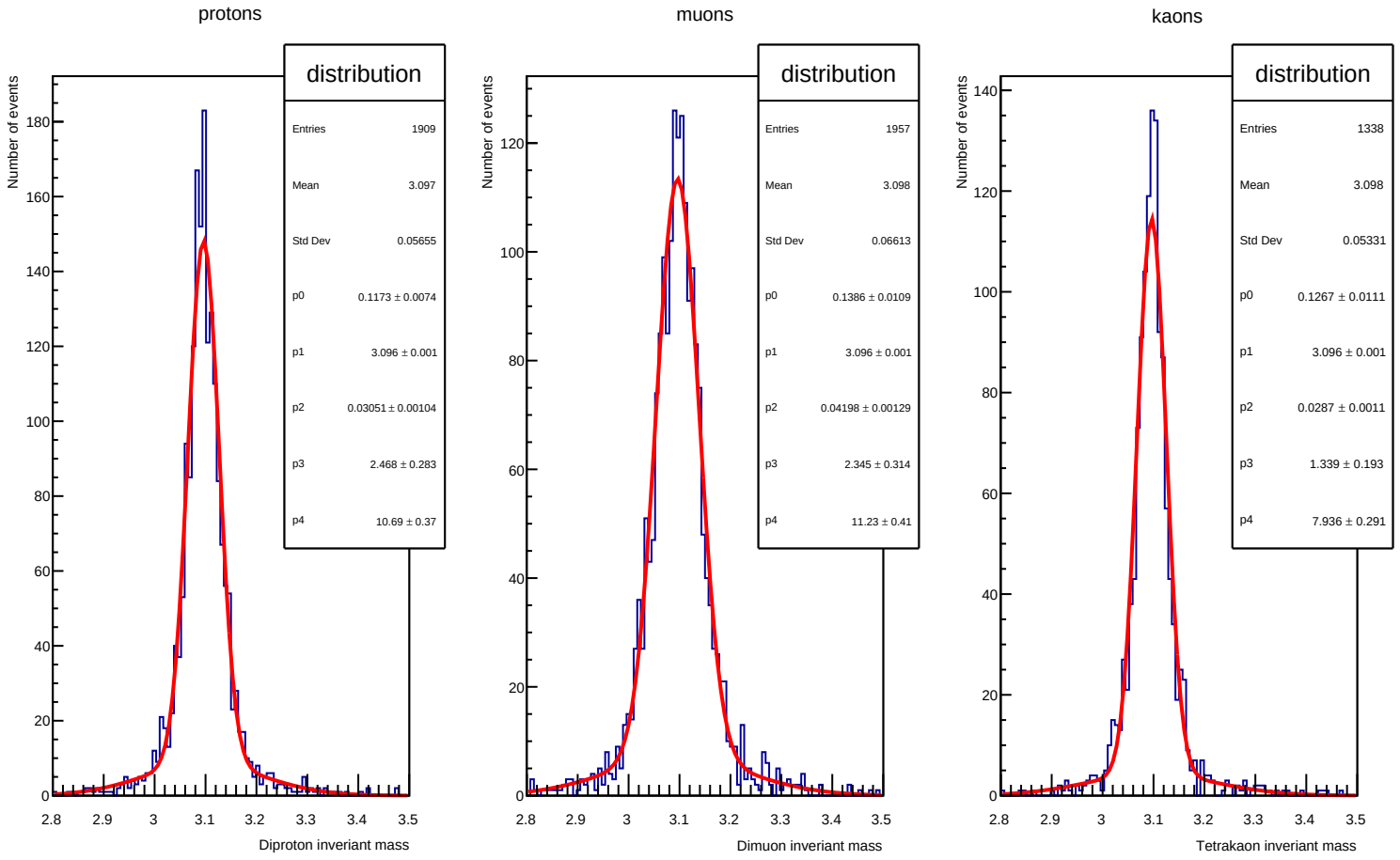

Рис. 17: Event distributions of $g + g \to J/\psi + g$ process with decays into different pairs. Fit parameter p_0 is width of first gaussian, p_2 - of second, p_1 is equal to mass and p_3 and p_4 - constant multipliers of first and second Gaussian

It is obvious that the $muon - antimuon$ distribution has a larger value of width than the $proton - antiproton$ distribution. The main reason for this is multiple scattering. [23] A charged particle passing through a medium is deflected by many small angle scatters. If we define

$$\theta_0 = \theta_{plane}^{rms} = \frac{1}{\sqrt{2}}\theta_{plane}^{rms} \tag{4}$$

then for many applications it is sufficient to use a Gaussian approximation for the central 98% of the

projected angular distribution, with a root mean square (rms) width given by the formula:

$$\theta_0 = \frac{13.6MeV}{\beta cp} z \sqrt{\frac{x}{X_0}} \Big[1 + 0.038 ln(\frac{xz^2}{X_0 \beta^2})\Big] \tag{5}$$

The width increases with increasing mass, and the distributions of protons and muons correspond to this information. Kaon decays have a very small width, which is not so obvious.

It was built distributions by βp form formula (5) to evaluate the contribution to the width of these values in the denominator normalized by the unit area under the graph. These distributions are shown in Figure 18. We can see similar distributions of protons and muons and there is still no answer to the question:"why dikaons-diantikaons distribution have such a narrow peak?

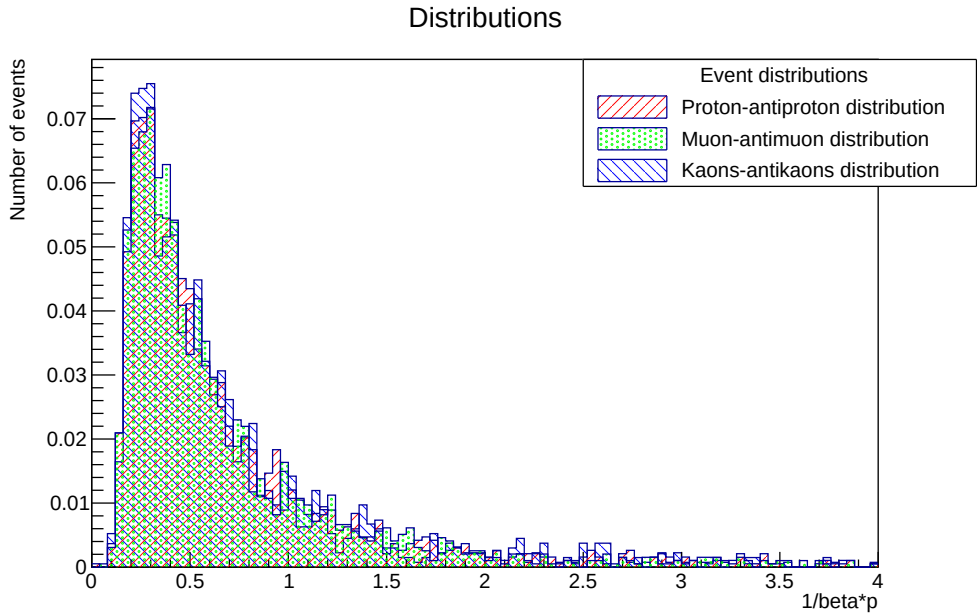

Рис. 18: Event distribution by $\frac{1}{\beta \cdot p}$

5.3 Signal-background for process $g + g \to J/\psi + g$

The main goal of this educational work is to build a signal-background picture of J/ψ production with decay to $p\bar{p}$ in SPDroot. For this purpose 3500 minimum bias events were generated.

For analysis after reconstruction a search for candidates for $p\bar{p}$ pair is necessary. To find these candidates, the results of track system reconstruction are used. There is "fitpars"method of MCTracks class to fit tracks back to primary vertex. In the final fitting point we can extract the momentum of the particle, but we still don't know "who"it is.

PID system is used for particle identifications. There are three main ways to separate candidates:

1. Energy losses, the mean rate of which for moderately relativistic charged heavy particles is described by the "Bethe equation":

$$\langle \frac{dE}{dx} \rangle = Kz^2 \frac{Z}{A} \frac{1}{\beta^2} \Big[\frac{1}{2} ln \frac{2m_e c^2 \beta^2 \gamma^2 W_{max}}{I^2} - \beta^2 - \frac{\delta(\beta\gamma)}{2}\Big]$$

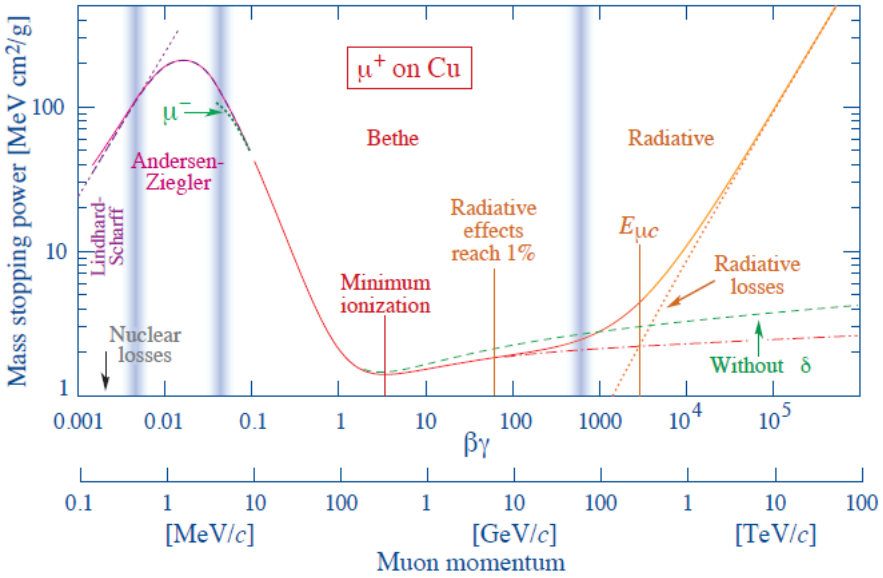

Рис. 19: Example of $\frac{dE}{dx}$ behavior for μ^+ with all effects and types of losses taking into account

2. TOF system, from which we have particle flight time. We can use so called "likelihoods which are probabilities of finding protons, kaons or pions from the proton candidate. These probabilities are found from a Gaussian-like probability density function for each candidate.
3. Aerogel, which was not used in this work.

The result of calculations is shown in figure 20. This result is not bad, but there are methods to reduce the signal to background ratio in SPDroot.

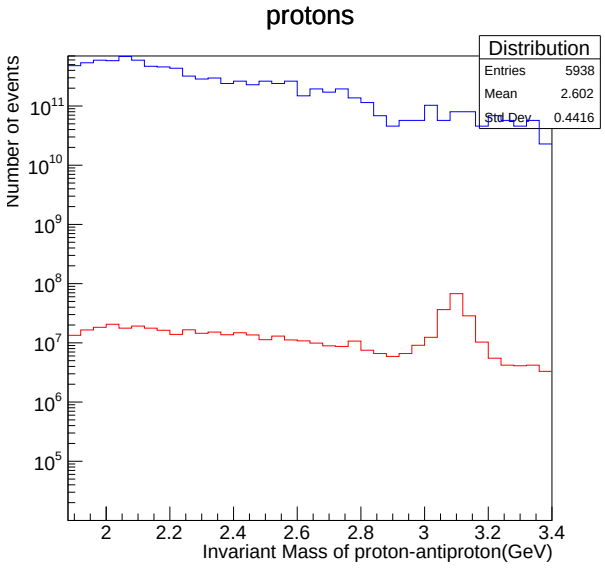

Рис. 20: First signal-background picture

5.4 Using PID information to improve the S/B ratio

To ensure that we have only candidates with large proton probabilities, strict restrictions have been placed on the likelihoods. A new signal-background plot with these restrictions is shown in Fig. 21.

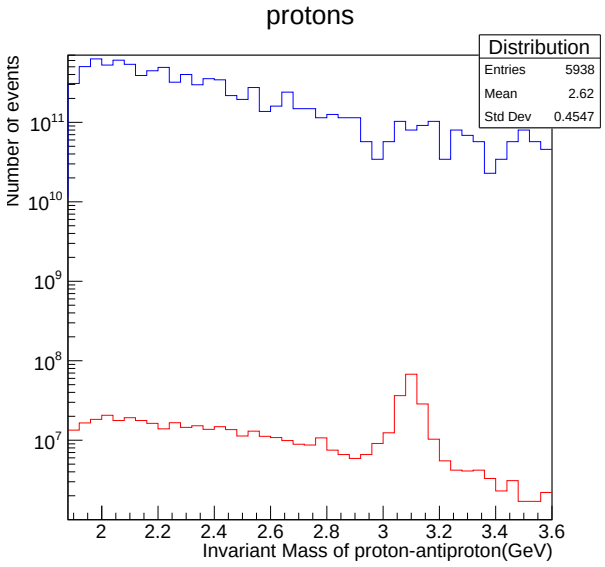

Рис. 21: Signal-background picture with strict restrictions on "Likelihoods"

True particle type was determined by MCTruth. Range of invariant masses [3.097-0.040 ; 3.097+0.040] (around the peak) is examined. Results of study of it in signal and background are shown in the table:

Number of pairs	Signal	Background
$p\bar{p}$	$985 \cdot 10^5$	$72 \cdot 10^{10}$
$\pi^+\pi^-$	0	0
K^+K^-	$1 \cdot 10^5$	0
$K^+\bar{p}$	$3 \cdot 10^5$	$6 \cdot 10^{10}$
π^+K^-	0	0
$\pi^+\bar{p}$	$2 \cdot 10^5$	0
pK^-	$2 \cdot 10^5$	$28 \cdot 10^{10}$
$K^+\bar{p}$	0	0
$p\pi^-$	0	0

We can see in the signal that we mostly have no chance to confuse with different types of particles, but we have big background contribution from pK^-. It is necessary to suppress the background correctly for more accurate identification.

5.5 Kinematic cuts to improve the S/B ratio

In addition to restrictions on the likelihoods, we can cut a region in phase space that is of interest to us with restrictions on, for example, the azimuthal angle of the particles. The number of events in the background is increased to 10500, because in the region around the peak there were not enough particles for a fair estimation.

There is uniform distribution for signal and pressed against the axis (because 0 and π angles at most particles).

In order to change the SB ratio, it was suggested to reduce the azimuthal angles for both protons and antiprotons by the function

$$f = \frac{1}{2(\pi - x)} - \frac{1}{2\pi}$$

This choice was dictated by the need for a hyperbolic-like constraint curve starting at the (0,0) point.

The azimuthal angle distribution for signal and background with the above mentioned sections is shown in Figures 22 and 23.

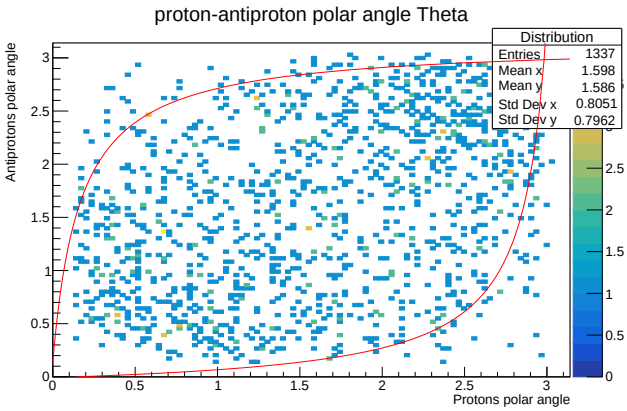

Рис. 22: Azimutal distributions of protons (on X axis) and antiprotons (on Y axis) in signal

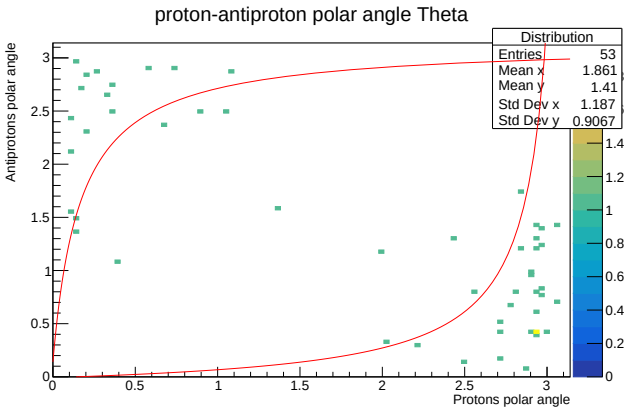

Рис. 23: Azimutal distributions of protons (on X axis) and antiprotons (on Y axis) in fon

Final signal-background picture with 21500 calculated events is shown on picture 24.

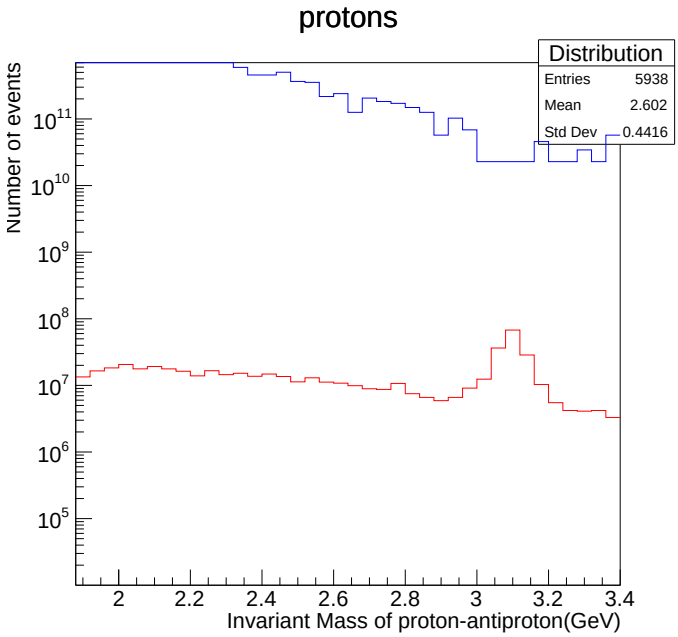

Рис. 24: Signal-background picture with cuts on "Likelihoods"and azimutal angles of proton-antiproton pairs

5.6 Event selection efficiency

The final task of this work is to evaluate the efficiency of the signal calculations. This distribution has to be fitted to find the correct number of events in the peak without background contribution.

The function $ax^2 + bx + c$ with a Gaussian distribution for a peak was chosen for fitting. The result is shown in Figure 25.

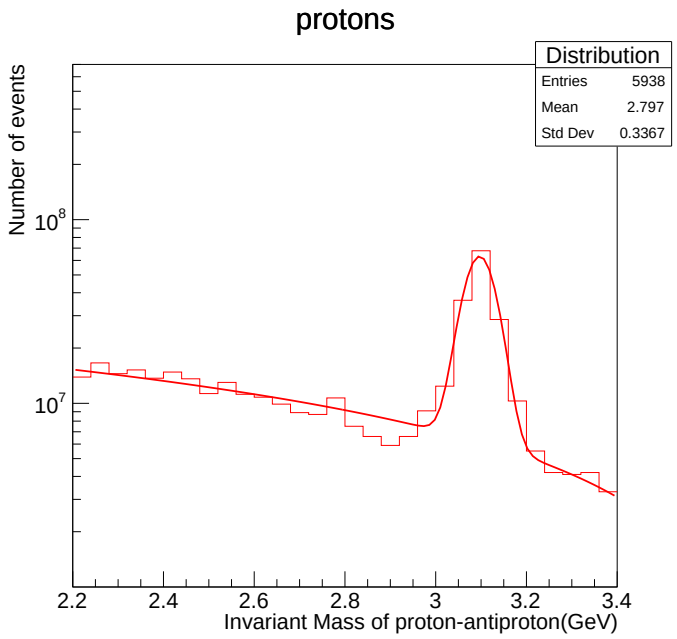

Рис. 25: Fitting of signal by sum of second degree polynomial and Gaussian distribution

After fitting, we can use the multiplicative constant of the Gaussian distribution (Gaussian normalised by 1 is used) without the quadratic polynomial, because it corresponds to the background, which we don't take into account in this task.

Final value of efficiency is 61.925%.

6 Summary

In this work, processes in Pythia8 were considered (all charmonia decay int pair of photons):

1. $g + g \to J/\psi + g$ with η_c parameters
2. $g + g \to \eta_c + g$ in inner J/ψ-production process in Pythia
3. $g + g \to \eta_c + g$ with creating corresponding class of Pythia
4. $g + g \to \eta_c$ with creating corresponding class of Pythia
5. $g + g \to \eta_c \to \gamma + \gamma$ with creating corresponding class of Pythia

In SPDroot some educational tasks were solved and I acquired skills:

— Simulating, reconstructing and analyzing of events in experiment
— Using MCParticles class to get information direct from Monte-Carlo generation in analyzis
— Finding tracks of particles and fitting them with "fitpars"method
— Particle identification
— Building distribution by momenta, angles, ivariant masses and others paramters
— Checking "Likelihoods"to separate real protons from other candidates
— Cut parts of phase space with restrictions on azimutal angles
— Fitting distribution to find some parameters of it
— Building Signal-Background distribution
— Separate Peak from background in signal distribution by event selection efficiency evaluation fit

7 Acknowledges

First of all, I would like to thank I.I. Denisenko and A.V. Guskov for their support and kind welcome. I would also like to express my gratitude to Pr. V.A. Saleev for his crucial guidance and assistance during this project. I would also like to express my gratitude to the Joint Institute for Nuclear Research for giving me the opportunity to participate in this programme. As JINR has been so fulfilling for me, I am very grateful for everything we have learnt there. Finally, I would like to thank the START Programme Coordinators, Ms Olga Korotchik and Ms Elena Karpova, for all their help.

References

[1] https://nica.jinr.ru/

[2] https://spd.jinr.ru/

[3] V. M. Abazod et al. Conceptual design of the Spin Physics Detector, https://doi.org/10.48550/arXiv.2102.00442

[4] B Abelev et al. Technical Design Report for the Upgrade of the ALICE Inner Tracking System. J. Phys. G, 41:087002, 2014.

[5] L. Glonti, T. Enik, V. Kekelidze, A. Kolesnikov, D. Madigozhin, N. Molokanova, S. Movchan, Yu Potrebenikov, and S. Shkarovskiy. Longitudinal tension and mechanical stability of a pressurized straw tube. Instruments, 2(4):27, 2018, 1810.04843.

[6] A. Arbuzov et al.,A. Arbuzov,On the physics potential to study the gluon content of proton and deuteron at NICA SPD, Progr. in Par. and Nuc. Phys., 119 (2021) 103858

[7] V. M. Abazov, G. D. Alexeev, Yu. I. Davydov, V. L. Malyshev, V. V. Tokmenin, and A. A. Piskun. Comparative analysis of the performance characteristics of mini-drift tubes with different design. Instruments and Experimental Techniques, 53(3):356–361, May 2010.

[8] Christian Bierlich et al. A comprehensive guide to the physics and usage of PYTHIA 8.3, https://doi.org/10.48550/arXiv.2203.11601

[9] https://pdg.lbl.gov/

[10] P. Cho and A.K. Leibovich, Color-octet quarkonia production II, Phys. rev. D, 53(11) (1995). https://pdg.lbl.gov/

[11] https://pythia.org/latest-manual/SemiInternalProcesses.html

[12] R. Gastmans, W. Troost, T.T. Wu, Cross-sections for gluon + gluon $\rightarrow$ heavy quarkonium + gluon// Phys. Lett. B 184 (1987) 257

[13] Д.В. Васин, В.А. Салеев. Адронное рождение тяжелых кваркониев в подходе квази-мульти-реджевской кинематики. // Вестник Самарского Государственного Университета, http://ssu.samara.ru/ vestnik/est/, 2005, № 6

[14] А.В. Ануфриев, В.А. Салеев. Рождение η_c с распадом в два фотона в обобщенной партонной модели при энергии коллайдера NICA //Вестник Самарского университета. Естественнонаучная серия. 2022. Том 28, № 1–2. С. 128–136

[15] T. Hahn, CUBA: a library for multidimensional numerical integration // Comput. Phys. Commun. 168 (2005) 78–95

[16] J. Collins, Foundations of Perturbative QCD (Cambridge Monographs on Particle Physics, Nuclear Physics and Cosmology, 32) Cambridge University Press (Cambridge, UK, 2011).

[17] A. Karpishkov, V. Saleev, M. Nefedo, Estimates for the single-spin asymmetries in the p↑p→J/ψX process at PHENIX RHIC and SPD NICA // Phys.Rev.D 104 (2021) 1, 016008

[18] R. Aaij et al., Measurement of the η_c(1S) production cross-section in pp collisions at $\sqrt{S}$=13 TeV, Eur. Phys. J. C80 (2020) 191

[19] https://git.jinr.ru/nica/spdroot

[20] https://fairroot.gsi.de/index.html

[21] https://geant4.web.cern.ch/

[22] https://root.cern/

[23] Prog. Theor. Exp. Phys. 2020, 083C01 (2020), https://pdg.lbl.gov/2021/html/computer_read.html